

MODELLING OF CH₄ PRODUCTION THROUGH THE DEPRESSURIZATION METHOD FROM BJØRNØYA GAS HYDRATE BASIN USING REACTIVE TRANSPORT SIMULATOR

Qorbani Kh.* and Kvamme B.

*Author for correspondence

Department of Physics and Technology,
University of Bergen,
Bergen, 5007,
Norway,

E-mail: khadijeh.qorbani@ift.uib.no

NOMENCLATURE

D	[m ² /s]	Diffusion coefficient
P	[MPa]	Pressure
R	[mol/(m ² s)]	Rate
T	[K]	Temperature
x, X	[1]	Mole-fraction
z	[nm]	Distance
H		Hydrate phase
β	[mol/kJ]	Inverse temperature $1/(RT)$
$\bar{\rho}$	[mol/m ³]	Molar density
μ	[kJ/mol]	Chemical potential
G	[kJ/mol]	Gibb's free energy.

ABSTRACT

Natural gas hydrates (NGHs) cannot reach thermodynamic equilibrium in real reservoir conditions. The enormous amount of methane stored in NGHs could be a potential source of energy. Lack of reliable field data makes it difficult to predict the production potential, as well as the safety of CH₄ production from NGHs. Computer simulations cannot substitute field data. Nevertheless, state of the art modelling can be used to evaluate possible long-term scenarios. However, we need proper kinetic models to describe hydrate dissociation and reformation and all phase transition routes must be considered. In this work, we utilized an in-house extension of RetrasoCodeBright (RCB) to perform a gas hydrate case study of the Bjørnøya basin, based on very limited geological data extracted from reported field studies. The aim of this research was to use a reactive transport simulator and non-equilibrium thermodynamics to analyse CH₄ production from the gas hydrate. Results show fast propagation of pressure drop wave throughout the reservoir layer by imposing drawdown pressure on the well, as a result, gas hydrate dissociation and CH₄ production started at the early stages of the five year simulation period.

INTRODUCTION

Hydrates are ice-like crystal structures of water containing trapped gas molecules (inside the cages formed by hydrogen bonded water molecules). Various hydrate formers in nature lead to different phases of hydrates. Thus, the combined first and sec-

ond law of thermodynamics and Gibb's phase rule imply that hydrates cannot reach thermodynamics equilibrium in nature. Due to this fact, there will be a competition between different hydrate phase transitions.

Natural gas hydrate occurrences are found in regions where at least temperature and pressure facilitates the formation of hydrate from natural gas components, like for instance in the permafrost and the continental margins. Total thermodynamic stability of these hydrates requires that the hydrate phase is the phase of lowest free energy for all components in the hydrate. This is normally hard to accomplish since there is always some fluid circulation on pore level and above, as a minimum diffusion in between hydrate and minerals. Normally it is therefore more correct to discuss the hydrate occurrences as being in a stationary state as trapped beneath clay, shale or other impermeable sealing structures.

Gas trapped inside the natural gas hydrates can have two different origins: gases with a biogenic source (that originate from natural decay of organic rich sediments) and gases with a thermogenic source (which, when leaking from deeper sources, is formed as a result of thermal maturation of organic substances) [1].

Due to the ever increasing demand for energy, new sources of energy are required worldwide. It is estimated that the amount of fuel gas that trapped inside the natural gas hydrate reservoirs could be twice the explored natural fossil fuels in the world [2]. The main hydrocarbon component inside NGH reservoirs is CH₄, as a result NGHs has attracted attention as a potential source of energy for the future.

Several conventional methods are proposed for productions of CH₄ from these reservoirs, such as pressure reduction, thermal stimulation and inhibitor-injection [3]. Recently, some new methods of CH₄ production has been proposed, such as CO₂ gas exchange through sequestration of CO₂ into NGHs reservoirs [4], microwave technology, fluorine gas and microwave technology [5]. However, apart from the economical point of view, it

has not yet been proven that application of these methods are safe enough in the long term. During production of CH₄ from natural gas hydrate reservoirs, the hydrate structure, which consists of water and gas, will dissociate and huge amounts of water will be associated with the produced gas. This may affect the geomechanical stability of the dissociating area and cause structural deformation.

In addition, the ongoing increase in the temperature at the bottom of the sea in the Arctic could destabilize the hydrate bearing sediments and release huge amounts of methane from the melting hydrate structure to the ocean and atmosphere. This phenomenon could potentially accelerate climate warming [6] (CH₄ is a greenhouse gas which is much more aggressive than CO₂).

The Bjørnøya basin is located in the south-west of the Barents sea. The inferred gas hydrate and free gas is located nearby or above large faults [1]. These faults control displacements of gas hydrates and free gases. The gas hydrate stability region is located close to the sea bed. Thus, the thickness of the gas hydrate is affected by a geothermal gradient, pore water salinity and water temperature at the seabed [7].

Gas leakage in this basin might be related to the Cenozoic evolution of the Barents Sea that caused removal of 1 km of sediments from the shelf of the basin, which in turn results in an expansion of gas and a tilting of the old reservoirs, thus releasing the gas [1]. Lithology of the area of accumulation of the gas hydrate and free gas in the Bjørnøya basin mostly consists of claystone and siltstone and to a lower degree sandstone. Thus, at the primary stages of gas migration, diffusion of gas as a result of the concentration gradient might be the dominant phenomenon [1]. Another possible stage of gas accumulation is the migration of gas in the form of bubbles or gas dissolved into water pores passing through fractures and faults towards the hydrate stability zone [1]. The total accumulation of gas hydrate in the Bjørnøya basin may cover an area of up to 55 km² [1].

Understanding the long term processes that may take place after initiating the production of CH₄ from NGHs is of high importance. Conducting field scale experiments are costly and time consuming. Therefore, using computer simulations to analyse several scenarios related to production and safety can be efficient both from a time perspective, as well as from an economic point of view.

Most hydrate simulators treat hydrate phase transitions using the equilibrium approach, while those that use the kinetic approach utilize simple laboratory derived formula like for example the Kim and Bishnoi laboratory scale method [8], which deviate severely from real reservoir conditions. Another limitation that can be found in all of today's hydrate simulators is that they only consider one route for hydrate phase transitions, which is towards water and hydrate formers in the gas phase (ignoring other possible routes). However, other routes do exist, for example, hydrate can also form from water and hydrate formers dissolved into the aqueous phase. Furthermore, hydrate can also form from hydrate formers adsorbed onto mineral surfaces.

The RetrasoCodeBright (RCB) hydrate simulator [9] has pre-

viously been modified to model CH₄ production using the depressurization method from natural gas hydrate reservoirs [10; 11]. Two different routes for hydrate phase transitions were implemented: hydrate formation, reformation and dissociation from hydrate formers inside the gas phase and hydrate formers inside the aqueous phase. A non-equilibrium thermodynamic package [12; 13; 14; 15] developed by our group was added to RCB, making it possible to account for competing hydrate phase transitions through minimization of Gibb's free energy changes. Nucleation theory was used as a primary step to relate mass and heat transfer contributions to the kinetic rate of hydrate phase transitions.

Today, the only NGH reservoir in the world that is producing gas is the Messoyakha field. However, the gas production data from this field is not accurate enough for history matching purposes.

In this work we have used RCB to examine the effects of our implementations in a case study of a real NGH reservoir located in the Bjørnøya basin. We briefly present our approach in the methods and procedures section and the interested reader can find a more detailed calculation and implementation method in Ref. [10] and [11], respectively. Simulation setup section contains the properties that we used to make the model. Results from our modifications are discussed in results and discussion section. Conclusions are made in the summary and conclusion section.

METHODS AND PROCEDURES

Even for a simple system of water and methane equilibrium cannot be established between three phases when temperature and pressure are both fixed by local conditions. This is of course trivial and the basis for all equilibrium measurements, in which only one of them is fixed. One consequence is that chemical potential of methane in different phases is not uniform and accordingly also hydrate created from methane as gas, as dissolved in water or as trapped in water structures on mineral surfaces will all result in different hydrate compositions and different unique phases by definition. The complexity of non-equilibrium increases with additional hydrate formers present in the system. As a result, equilibrium could not be reached and there is always a competition between the various hydrate formers. Thus, at each time step and each node only those hydrate phase transitions that yield a minimum free energy change have the possibility to occur. A realistic modelling of NGHs requires taking into account all of the various routes of phase transitions by considering the competition between all presenting hydrate formers using Gibb's free energy minimization. Previously, two routes for methane hydrate phase transitions were implemented into RCB using the reactions $\text{CH}_4^{(\text{gas})} + 5.75 \text{H}_2\text{O}^{(\text{liq.})} \rightarrow (\text{Hydrate})^1$, and $\text{CH}_4^{(\text{aq.})} + 5.75 \text{H}_2\text{O}^{(\text{liq.})} \rightarrow (\text{Hydrate})^2$. The interested reader can find detailed calculations and implementation methods in Ref. [10; 11]. The following description is the methodology that we have used in implementing the second route where guest molecule is CH₄^(aq.). At this stage we used classical nucleation theory to calculate the kinetic rate of hydrate phase transitions.

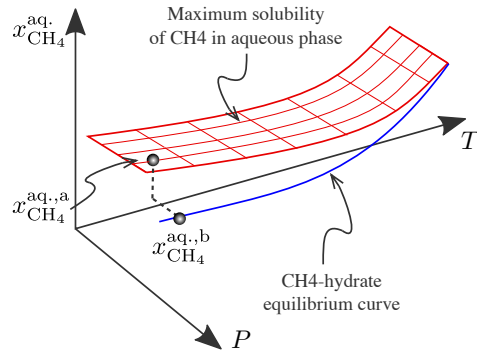


Figure 1. The maximum CH_4 solubility into aqueous phase (red surface) and the minimum soluble CH_4 inside the aqueous phase that is required to keep hydrate stable (blue line)

Through nucleation theory it is possible to relate mass transfer, heat transfer and non-equilibrium thermodynamic calculations to the kinetic rate of hydrate phase transitions:

$$R(i, t, n) = R_0 \cdot e^{-\beta \Delta G}, \quad (1)$$

where $R(i, t, n)$ is the dissociation/formation/reformation rate of hydrate type i in node number n at time step t . R_0 is the mass transport controlling term that is calculated using Fick's Law. In the CH_4 -hydrate system water is the dominant component and it always exists in the environment. As a result mass transport of CH_4 inside the aqueous phase is the constraint for phase transitions. Thus, we have that $R_0 = -D \cdot \bar{\rho} \cdot \partial X / \partial z$, where R_0 is the mean value of the CH_4 diffusive flux at the hydrate and water interface. $\partial X / \partial z$ is the CH_4 mole fraction gradient from the hydrate surface to the interface. $\bar{\rho}$ is the methane hydrate molar density that is equal to 949.4 mol/m^3 .

A non-equilibrium thermodynamic package that is developed within our group was added to RCB [12; 13; 14; 15]. Using this package made it possible to define the constraints of the system with respect to thermodynamic variables. To determine which hydrate phase transitions are likely to occur for every node at every time step, ΔG of each phase transition is calculated based on independent thermodynamics variables, namely pressure, temperature and concentration of $\text{CH}_4^{(\text{aq.})}$. Then, we ignore those hydrate phase transitions with positive ΔG and those which are unlikely with $\Delta G_s < \varepsilon$, thus taking into account only those phase transitions that have negative enough free energy changes to pass the barrier of nucleation. The free energy change is

$$\Delta G = \delta [x_w^H (\mu_w^H - \mu_w^{(\text{aq.}),a}) + x_{\text{CH}_4}^H (\mu_{\text{CH}_4}^H - \mu_{\text{CH}_4}^{(\text{aq.}),a})],$$

where ΔG in this formula is calculated for every hydrate phase transition. δ will become $+1$ for hydrate formation and -1 for hydrate dissociation. The superscripts H and (aq.) denotes hydrate and aqueous phases. Superscript (a.) denotes the mole frac-

tion of $\text{CH}_4^{(\text{aq.})}$ in Fig. 1 at given pressure and temperature conditions in the specific node.

Whether the aqueous phase is supersaturated or undersaturated with respect to the hydrate former, $\text{CH}_4^{(\text{aq.})}$, depends on the $\text{CH}_4^{(\text{aq.})}$ concentration at given pressure and temperature in every node and every time step. A concentration of $\text{CH}_4^{(\text{aq.})}$ that lies above the blue line and below the red plane in Fig. 1, implies that the aqueous phase is supersaturated with respect to $\text{CH}_4^{(\text{aq.})}$. Thus hydrate formation will take place according to the kinetic rate that is defined in Eq. (1). If the specific area in the reservoir model comes into contact with brine water that is undersaturated with respect to CH_4 then the $\text{CH}_4^{(\text{aq.})}$ concentration in Fig. 1 lies below the blue line and the hydrate will start to dissociate.

SIMULATION SETUP

Gas hydrate at Bjørnøya overlays a gas zone. The gas has a thermogenic source [16] and has migrated from deeper sources. To simulate gas production from this basin, we constructed a two-dimensional model shown in Fig.2. The length and thickness of the model were 1000 m and 300 m, respectively. We divided the model into 300 elements with equal sizes of $20 \text{ m} \times 10 \text{ m}$. The model consists of three layers, with a sealing layer at the top, a hydrate layer in the middle and an underlying gas layer.

The average water depth in the Barents sea is about 230 m, while inferred gas hydrate occurrence takes place at a water depth of 400 m [16]. Thus, the top of the caprock in the model is located at a water depth of 400 m. The location of the assigned production well is 10 m below the hydrate layer inside the gas layer. Production pressure of the well was set to 4.5 MPa, which is outside of the CH_4 -hydrate stable region of that specified node. The gas hydrate stability zone increases exponentially with the water depth up to 500 m and after that depth the increase in stability zone turns to be gradually [7].

Unconsolidated sediments spread along the young continental margins in the west [17]. Due to the mineralogy of Bjørnøya basin [1] and since we could not find any representative data for permeability of the hydrate layer and the gas layer, thus we utilized the unconsolidated siltstone and very fine sandstone permeabilities and set them equal to $3 \cdot 10^{-15} \text{ m}^2$ for the hydrate layer and $2 \cdot 10^{-14} \text{ m}^2$ for the gas layer.

The average density and porosity are estimated to be equal to 2150 kg/m^3 and $\phi = 30 \%$, respectively, while the maximum and minimum hydrate saturation are expected to be between 47% and 26% [16]. Thus, the highest and the lowest hydrate in-situ volume will be between $3.8 \cdot 10^8 \text{ m}^3$ and $1.9 \cdot 10^8 \text{ m}^3$, respectively [16]. For our model we used the minimum hydrate saturation value. In the Barents sea the geothermal gradient is varying [7] and its average is approximately $0.03 \text{ }^\circ\text{C/m}$ [1]. The pressure gradient is estimated to be 0.01 MPa/m [1].

Average bottom water temperature in the Barents sea is affected by different water mass movements [18]. The main water masses consists of cold water from the Arctics and the warm water from the Atlantic sea. At the cold water mass boundary the temperature varies between $-1.5 \text{ }^\circ\text{C}$ to $5 \text{ }^\circ\text{C}$ from the bottom to

the top, while in the warm water region it varies from 2 °C to 10 °C. The variation in temperature between summer and winter time is negligible [7]. The bottom sea temperature is approximately 2° C [1]. The thickness of the hydrate stability zone is varying from approximately 155 m at areas that water depth is 395 m to 170 m where water depth is 440 m [1]. The thickness of the hydrate layer is estimated to be approximately 110 m in this paper.

Initial pressure, temperature and mean stress, were set to 4 MPa, 275.15 K and 8.97 MPa, respectively for the top boundary, while for the bottom boundary they were set to 7 MPa, 285.65 K and 15.4 MPa, respectively. Initial hydrate saturation was 0.26. Reservoir properties and material properties that were used to model the Bjørnøya gas hydrates are listed in Table 1 and Table 2. Chemical primary species in the aqueous phase were set to H₂O, HCO₃⁻, OH⁻ and O₂^(gas), while chemical secondary species were CH₄^(aq.), CO₃²⁻, H⁺ and CO₂^(aq.). In the gas phase we had CH₄^{gas}. The model was run for 5000 time steps, which is equivalent to a 5 years time span.

RESULTS AND DISCUSSION

CH₄ production from the assigned production well started at time zero. Temperature and pressure of the production well were set to values outside the stability region of the gas hydrate. Pressure difference between the production well and its surroundings is the main driving force for dissociation of hydrate to initiate. As it is clear from Fig. 3, pressure draw down propagated rapidly throughout the entire hydrate layer.

Hydrate phase transitions were tracked through porosity changes. As a result of rapid pressure drops propagating throughout the entire reservoir, the complete hydrate layer was driven outside the stability region at the early stages of simulation, thus causing hydrate to dissociate. The increase in porosity is depicted in Fig. 4. Gas flux towards the production well from the

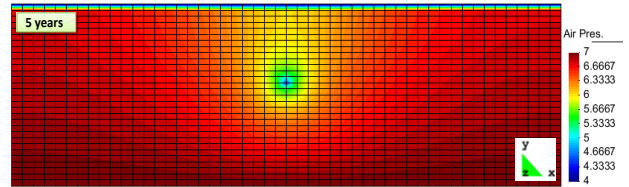


Figure 3. Pressure changes after 5 years of production.

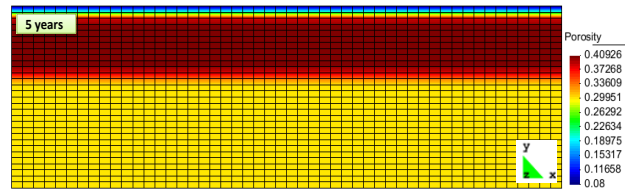


Figure 4. Porosity changes inside the reservoir after 5 years of production.

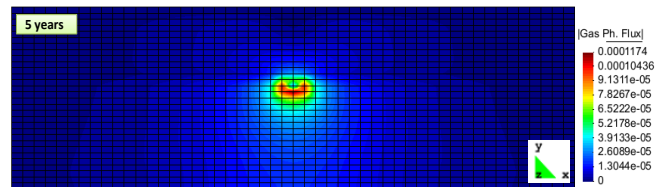


Figure 5. CH₄ gas flux inside the reservoir after 5 years of production.

gas layer and the hydrate layer is shown in Fig. 5. Heat transfer is the controlling mechanism of methane hydrate dissociation, which is an endothermic process that adsorbs heat from its surroundings. Fig. 6 shows heat flux in the model. As it is clear from Fig. 7, temperature of the reservoir decreased continuously. In the layer that contains gas, reduction of temperature due to gas expansion is clearly visible.

The strength of the hydrate bearing sediments is affected by the strain rate, consolidation stress, grain size, temperature, den-

Property	G	H	C
Young's modulus [GPa]	0.5	0.5	0.5
Poisson's ratio	0.25	0.25	0.25
Zero stress porosity	0.3	0.3	0.08
Zero stress permeability [m ²]	2·10 ⁻¹⁴	3·10 ⁻¹⁵	10 ⁻³⁵
Van Genuchten's gas entry pressure (at zero stress)	0.0196	0.0196	0.196
Van Genuchtens exponent [m]	0.457	0.457	0.457
Longitude dispersion factor [m]	11	11	11
Molecular diffusion [m]	10 ⁻¹⁰	10 ⁻¹⁰	10 ⁻¹⁰

Table 1. Properties of the reservoir model layers, where G denotes the gas layer, H denotes the hydrate layer and C the cap rock layer.

Property	Value	Unit
Thermal conductivity of saturated medium	2.18	W/(m·K)
Thermal conductivity of dry medium	2.0	W/(m·K)
Solid Phase Density	2150	Kg/m ³
Specific heat of rock	874	J/(kg·K)
CH ₄ -hydrate molecular weight	119.5	g/mol
CH ₄ -hydrate density	907.40	kg/m ³
CH ₄ -hydrate specific heat	2200	J/(kg·K) [19]
CH ₄ -hydrate reaction enthalpy	53.24	kJ/mol

Table 2. Medium Properties

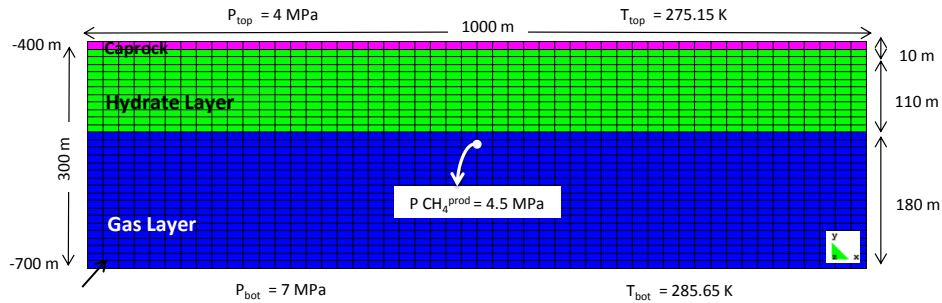


Figure 2. The reservoir model with one production well

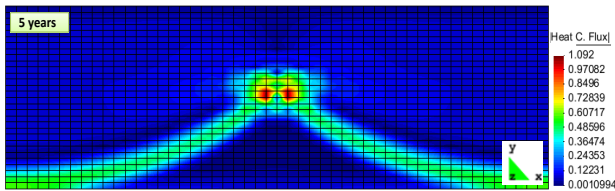


Figure 6. Heat flux inside the reservoir after 5 years of production.

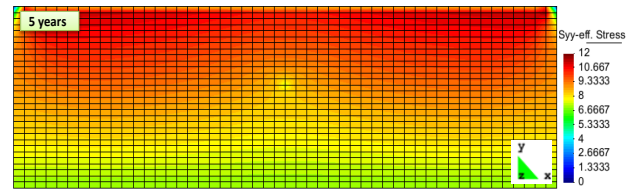


Figure 8. Effective stress in Y-direction after 5 years of production.

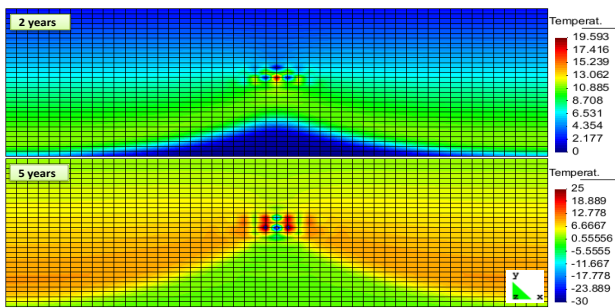


Figure 7. Temperature after 2 and 5 years of production.

sity and cage occupancy [20]. Hydrate, as a pseudo mineral, is part of the matrix and hydrate saturation above 25-40 % can contribute in bearing of the overburden stress of the top layers [21]. Dissociation of hydrate reduces the matrix volume that carry the load. Thus, effective stress becomes the dominant mechanism that controls the sediment stiffness and strength [21]. Furthermore, during production of CH_4 from hydrate reservoirs, the pore pressure will drop gradually and the net compaction pressure on the matrix increases. Therefore, the stability of the dissociated area will be affected and may cause compaction and destruction of the local structures. Inside RCB geomechanical effect of hydrate dissociation from hydrate bearing sediments was performed implicitly and carried out applying geomechanical calculations at the same time step that flow calculations were performed. Fig. 8 shows effective stress in the vertical direction. Due to lack of tensile strength data of the hydrate layer in Bjørnøya, it was not possible to analyse the possibility of collapse and compaction of the structure.

SUMMARY AND CONCLUSIONS

We applied the RCB hydrate simulator [9] to conduct a case study on pressure reduction triggered production of natural gas

based on geological data from the Bjørnøya hydrate reservoir [1]. The current version of the hydrate simulator utilizes a reactive transport algorithm to minimize free energy locally for calculations of most likely phase distributions in a non-equilibrium system. The advantage of this platform is that each of the competing hydrate phase transitions can be modelled as pseudo reactions and then be treated as non-equilibrium reactions subject to the free energy minimization algorithm. In every time step the solver has an implicit algorithm for solving mass flow, heat flow and geomechanics. The mass flow is then, in the same time step, correcting for changes in phase distributions of all components over all possible phases and returns the individual mass fluxes of all components back to the next time step of the primary solver. Kinetic rates of hydrate dissociation and reformation were calculated within RCB using classical nucleation theory. Competing phase transitions of two possible hydrate routes were calculated using a non-equilibrium thermodynamic package developed by our group and added to RCB.

Results show that the pressure drop imposed through the production well propagated rapidly throughout the reservoir. This may be due to the high permeability of both the hydrate and the gas layers, resulting in a better connection between pores inside the medium. Thus, methane hydrate dissociation from the hydrate layer starts at the early stages of simulation.

Gas hydrate at Bjørnøya consists of loose fine-grained sediment. Thus, hydrate occurrence might be spread in the sediment, forming veins and nodules [21]. Consideration of sand production due to hydrate dissociation can also be of importance for this basin. A sensitivity study on critical parameters like permeability, porosity, inhomogenities and initial mechanical strength of the hydrate filled sediments is needed in order to get a better picture of the hydrate production potential.

Lack of specific data on flow parameters and initial mechan-

ical strength of the sediments containing the hydrate is a limitation for quantitative interpretations of the simulation. A sensitivity study on critical model parameters for the actual conditions is planned.

ACKNOWLEDGEMENTS

We acknowledge the grant and support from Research Council of Norway and Industrial partners through the following projects: CLIMIT "Safe long term sealing of CO₂ in hydrate", Research Council of Norway, project number: 224857, SSC-Ramore, "Subsurface storage of CO₂ - Risk assessment, monitoring and remediation", project number: 178008/130, FME-SUCCESS, project number: 804831, PETROMAKS, "CO₂ injection for extra production", Research Council of Norway, project number: 801445, PETROMAKS "CO₂ Injection for Stimulated Production of Natural Gas", Research Council of Norway, project number: 175968 and 230083, STATOIL, under contract 4502354080.

REFERENCES

- [1] Laberg, J. S., and Andreassen, K., Gas hydrate and free gas indications within the Cenozoic succession of the Bjørnøy Basin, western Barents Sea. *Marine and Petroleum Geology*, Vol.13, 921–940, 1996. doi=10.1016/S0264-8172(96)00038-4
- [2] Kvenvolden, K.A., Gas hydrates as a potential energy resource - a review of their methane content, in D. G. Howell, ed., *The Future of Energy Gases - U.S. Geological Survey Professional*, Washington, United States Government Printing Office, Paper 1570, 555–561, 1993.
- [3] Sloan, E.D. and Koh, C., Clathrate Hydrates of Natural Gases, 3rd ed, *CRC Press*, 2007, USA.
- [4] Graue, A., Kvamme, B., Baldwin, B., Stevens, J., Howard, J., Aspenes, E., Ersland, G., Husebo, J. and Zornes, D., MRI Visualization of Spontaneous Methane Production From Hydrates in Sandstone Core Plugs When Exposed to CO₂, *SPE Journal*, Vol.13, 146–152, 2008, doi=10.2118/118851-PA.
- [5] Arora, A., Cameotra, S.S., Balomajumder, C., Techniques for Exploitation of Gas Hydrate (Clathrates) an Untapped Resource of Methane Gas. *Journal of Microbial and Biochemical Technology*, Vol.07, 108–111, 2015, doi=10.4172/1948-5948.1000190.
- [6] Chabert, A., Minshull, T. A., Westbrook, G. K., Berndt, C., Thatcher, K. E., and Sarkar, S., Characterization of a stratigraphically constrained gas hydrate system along the western continental margin of Svalbard from ocean bottom seismometer data. *Journal of Geophysical Research*, Vol.116, B12102, 2011, doi=10.1029/2011JB008211.
- [7] Chand, S., Mienert, J., Andreassen, K., Knies, J., Plassen, L., and Fotland, B., Gas hydrate stability zone modelling in areas of salt tectonics and pockmarks of the Barents Sea suggests an active hydrocarbon venting system. *Marine and Petroleum Geology*, Vol.25, 625–636, 2008, doi=10.1016/j.marpetgeo.2007.10.006.
- [8] Kim, H. C., Bishnoi, P. R., Heidemann, R. A., and Rizvi, S. S. H., Kinetics of methane hydrate decomposition. *Chemical Engineering Science*, 42, 1645–1653, 1987, doi=10.1016/0009-2509(87)80169-0.
- [9] Saaltink M.W., Ayora C., and Olivella S., User's guide for RetrasoCodeBright (RCB), *Institute of Earth Sciences Jaume Almera, Spanish Research Council (CSIC), Barcelona, Spain*, V 1.2, 2008, URL <http://h2ogeo.upc.edu/software/ManualRCB.pdf>.
- [10] Qorbani, Kh., and Kvamme, B., Non-equilibrium simulation of CH₄ production through the depressurization method from gas hydrate reservoirs, *Journal of Natural Gas Science and Engineering*, 2016, doi=10.1016/j.jngse.2016.03.102.
- [11] Chejara, A., Kvamme, B., Vafaei, M. T., and Jemai, K., Simulations of long term methane hydrate dissociation by pressure reduction using an extended RetrasoCodeBright simulator. *Energy Conversion and Management*, Vol.68, 313–323, 2013, doi=10.1016/j.enconman.2012.09.003
- [12] Kvamme, B., Kinetics of Hydrate Formation From Nucleation Theory, *International Journal of Offshore and Polar Engineering*, Vol.12, 256–263.
- [13] Kvamme, B., Droplets of Dry Ice And Cold Liquid CO₂ For Self Transport of CO₂ to Large Depths, *International Journal of Offshore and Polar Engineering*, Vol.13, 139–146.
- [14] Kvamme, B., Kuznetsova, T., Kivelä, P.-H., and Bauman, J., Can hydrate form in carbon dioxide from dissolved water? *Physical Chemistry Chemical Physics*, Vol.15, 2063–2074, doi:10.1039/c2cp43061d.
- [15] Kvamme, B., Qasim, M., Baig, K., Kivelä, P.-H., and Bauman, J., Hydrate phase transition kinetics from Phase Field Theory with implicit hydrodynamics and heat transport. *International Journal of Greenhouse Gas Control*, Vol.29, 263–278, 2014, doi=10.1016/j.ijggc.2014.08.003.
- [16] Laberg, J. S., Andreassen, K., and Knutsen, S.-M. Inferred gas hydrate on the Barents Sea shelf- a model for its formation and a volume estimate. *Geo-Marine Letters*, Vol.18, 26–33, 1998, doi=10.1007/s003670050048.
- [17] Knutsen, S.-M., and Vorren, T. O., Early Cenozoic sedimentation in the Hammerfest Basin. *Marine Geology*, Vol.101, 31–48, 1991, doi=10.1016/0025-3227(91)90061-8.
- [18] Løvhø, V., Elverhøi, A., Antonsen, P., Solheim, A., and Liestøl, O., Submarine permafrost and gas hydrates in the northern Barents Sea, *Norsk Polarinstitutt*, 1990, Retrieved from http://id.tjeneste.nb.no/URN:NBN:no-bibsys-brage_13220
- [19] Waite, W. F., Stern, L. A., Kirby, S. H., Winters, W. J., and Mason, D. H., Simultaneous determination of thermal conductivity, thermal diffusivity and specific heat in SI methane hydrate. *Geophysical Journal International*, Vol.169, 767–774, 2007, doi=10.1111/j.1365-246X.2007.03382.x.
- [20] Winters, W. J., Pecher, I. A., Waite, W. F., and Mason, D. H., Physical properties and rock physics models of sediment containing natural and laboratory-formed methane gas hydrate. *American Mineralogist*, Vol.89, 1221–1227, 2004, doi=10.2138/am-2004-8-909.
- [21] Waite, W. F., Santamarina, J. C., Cortes, D. D., Dugan, B., Espinoza, D. N., Germaine, J., and Yun, T.-S., Physical properties of hydrate-bearing sediments, *Reviews of Geophysics*, Vol.47, RG4003, 2009, doi=10.1029/2008RG000279